

II PROTECTION OF STEEL PIPELINES FROM PERMANENT GROUND DEFORMATION USING EPS GEOFOAM

Steven F. Bartlett
Bret N. Lingwall
Aurelian C. Trandafir
Evert C. Lawton

INTRODUCTION

This chapter discusses the application, design and construction of EPS geofoam for protecting buried pipelines against vertical and horizontal displacement resulting from permanent ground deformation. The concept of using EPS as a compressible inclusion and as a lightweight cover system is evaluated for buried steel pipeline applications.

EPS Geofoam Applications and Manufacturing

Expanded polystyrene (EPS) geofoam is a type of cellular geosynthetic used in both above and below ground applications in civil engineering (Figure 1). Its primary applications are: ultra-lightweight fill, compressible inclusions, noise and vibration damping, and thermal insulation of pavements (Horvath, 2001). The process for manufacturing EPS was developed in the 1950s, and the first below ground application was the insulation of foundation walls for residential housing in Scandinavia during the 1960s. In addition, geofoam has been placed under pavements in Scandinavia, Canada and the United States to prevent seasonal freeze-thaw. In the 1970s, EPS embankment construction using geofoam blocks was introduced as an ultra-lightweight fill in the United States and Norway to reduce settlement and improve bearing capacity of roadways (Horvath, 1995). Most notably in 1972, the Norwegian Road Research Laboratory (NRRL) placed geofoam blocks in the approach fill of the Flom Bridge to reduce differential between the approach and bridge (Aaboe, 2000). Since that time, NRRL continued research and long-term monitoring programs at this and others locations. Such studies have greatly added to the understanding of EPS and its long-term performance (Aaboe, 2000).

Although EPS block are referred to in this article as “geofoam,” other types of polystyrene have been used to manufacture geofoam block (Horvath, 1995). EPS block are created during a two-stage process. In the first stage, tiny polystyrene resin beads are expanded using a hydrocarbon-blowing agent (i.e., pentane gas) that is contained within each bead. During this stage, the beads are exposed to steam causing a softening of the resin and the subsequent expansion of the bead by the pentane gas. This creates a cellular structure within each bead which is called “pre-puff.” After a short stabilization period, the pre-puff is placed in a large block mold and steam is injected causing additional expansion and the beads coalesce. The result, upon cooling, is a relatively solid block of light-weight material that has a closed, air-filled, cellular structure. Individual cells (i.e., remnants of the beads) are still visible after the block molding process, but the beads have so completely coalesced to form a closed fabric with essentially no void between the cells.

Block molds typically produce geofoam block that ranges from 500 to 600 mm high, 1000 to 1200 mm wide and 2000 mm to 5000 mm long (Horvath, 1996a) (Figure 1). Geofoam block can be hot-wire cut at the manufacturing plant or cut by hand in the field to the required size and shape during block installation

GENERAL DESIGN AND CONSTRUCTION CONSIDERATIONS

EPS Density

The density of the selected EPS is an important design consideration engineering applications. EPS compressive and shear strength, modulus and post-yield behavior are strongly correlated with density where strength and stiffness increase with increasing density, as discussed later. Commonly manufactured EPS densities (kg/m^3) are: EPS12, EPS15, EPS19, EPS22, EPS29, EPS39 and EPS46, where EPS12 represents a mass density of 12 kg/m^3 , etc.

Solvent, Fire and Insect Protection

Geofoam must be protected from potential spills of petroleum based fuels and solvents (e.g., gasoline and diesel fuel) and from fire. The overlying pavement section and trench backfill are the primary protection against such spills. However, a geomembrane liner can be used to provide additional protection, if deemed necessary. Typically a tri-polymer membrane, consisting of polyvinyl chloride, ethylene interpolymer alloy, and polyurethane or a comparable polymer combination is used. A modified flame retardant resin may be also added to the EPS for fire protection. Also, borate additives prevent insect attacks and boring intrusion.

Water Absorption and Buoyancy

When placed underground, EPS absorbs water in two ways. First, water will enter voids between the beads, or cells, due to capillary rise. Second, water vapor may diffuse into the cells when a temperature gradient exists and later condense when the temperature decreases below the dew point. For projects where the geofoam will be placed at or near the water-table, long-term studies from Norway give valuable performance data and design guidance for water absorption (Aaboe, 2000). In summary, the study showed that samples retrieved from EPS blocks placed in drained conditions (i.e., permanently installed above water-table) had water contents of 1 percent, or less. For blocks that were periodically submerged, water contents reached up to 4 percent by volume; and blocks that were permanently submerged, water contents reached values approaching 10 percent by volume (Aaboe, 2000). Current Norwegian design practice is to use a design unit weight of 0.5 kN/m^3 for the drained case and a design unit weight of 1.0 kN/m^3 for both the periodically and permanently submerged cases (Aaboe, 2000). This corresponds to an approximate design water content of 5 and 10 percent for the drained and submerged (e.g., periodic and permanent) cases, respectively, which appears to be reasonably conservative based on the retrieved samples.

Because of its light-weight nature, geof foam can also experience large uplift forces when submerged. Norway has experienced a case where a geof foam supported highway literally floated when a flood inundated the roadway constructed atop EPS (Aaboe, 2000). To counter the buoyant force, the amount of earthen material placed atop the geof foam must be increased over that of the dry case. For the case of complete submersion, the design uplift force per unit submerged volume is about 9.6 kN/ m^3 . To counteract this buoyant force, Horvath (1995) recommends increasing the overburden weight atop the geof foam, until a factor of safety of 1.3 is obtained for water levels corresponding to a 100 year design flood event. If the depth of overburden is increased to counteract buoyancy, the designer should also ensure that the applied dead load does not exceed more than 30 percent of the compressive strength of the geof foam. Also, it is important to provide a well-drained sand layer behind and underneath geof foam for areas that are constructed into hillsides. Downslope groundwater flow should not be allowed to impound behind the geof foam mass, which could produce lateral pressures on the geof foam blocks, potentially moving the geof foam mass laterally.

Long-Term Performance

Based on monitoring in Norway, the material properties of geof foam do not appear to degrade significantly with time (Aaboe, 2000). Norwegian practice requires a minimum compressive strength of 100 kPa for newly placed geof foam. To measure any potential degradation with time, Aaboe (2000) postulates that any significant loss of compressive strength would indicate deterioration. To this end, the Norwegian Road Research Laboratory has exhumed and carried out strength testing on samples which have been underground for durations ranging from 4 to 24 years. Unconfined compressive strength for these samples ranged from 105 kPa to 130 kPa, with no distinct trend of decreasing compressive strength with age. Aaboe (2000) attributes most of the variation in geof foam strength to variations in geof foam quality at placement, and not to any degradation with time. Further, there was no sign of variation in compressive strength based on whether or not the retrieved samples were wet or dry. This suggests that water absorption has no affect on compressive strength.

Cost

Geof foam blocks are more costly than earthen materials when considered on a unit volume basis. Because EPS is a plastic, its unit price fluctuates with petroleum costs and the density of the installed EPS for the particular application. Blanket cost comparison between geof foam and earthen fills and trench materials can be misleading. Each situation requires a review of the conditions and geometry before costs can be compared. Beyond the easily determined direct costs, less tangible costs must also be considered. Potential improved life cycle costs to overlying pavements, reduced construction time, elimination of utility relocation costs must be included in the cost evaluation.

EPS PROPERTIES AND BEHAVIOR

The selection of EPS for buried applications requires knowledge of its physical properties and how these properties vary as a function of EPS density, strain rate and strain range. These properties will be summarized for EPS densities commonly used in trenches that must support overlying streets and roadways.

Compressive Strength and Young's Modulus

Many research and EPS manufactures have performed laboratory testing on 50 mm cube samples of EPS to determine its elastic properties. Typical stress-strain curves for unconfined compression of 50-mm cubic samples of EPS19 are shown in Figure 2 (Bartlett et al. 2000). The initial strain lag seen in these curves is due to uneven contact during initial loading and the corresponding moduli were adjusted. The corrected Young's moduli for these tests range from 2.9 to 5.1 MPa. These data also show that EPS19 reaches yield (i.e., plastic behavior) at an axial strain of about 2 percent (Figure 2). In addition, the compressive resistance at 5 and 10 percent strain are, on average, 97 and 111 kPa, respectively.

For the most part, much of what is commonly known about EPS Young's modulus is based on data derived from unconfined compression testing of standard 50-mm cube samples. However, performance observations of EPS block placed in field applications suggest that Young's modulus values derived from laboratory tests when used in numerical analysis tend to overestimate the field measured deformations (Elragi 2000; Negusse et al. 2001; Newman et al. 2008.). It is clear that Young's modulus values determined from relatively small samples (i.e., 50 mm cubes) generally underestimate the true values obtained from large block samples (Elragi 2000; Elragi et al. 2000). Testing on full-sized EPS19 geofabric block has yielded moduli values as high as 14 MPa (Elragi, 2000); however, a more typical value is about 10 MPa (Elragi 2000; Negusse et al. 2001; Newman et al. 2008). The underestimation of the true Young's modulus attributed to 50-mm cube sample testing is probably due to end and edge effects that unduly influence the moduli results; thus, testing of larger samples is preferred for developing design and construction acceptance criteria (Elragi et al. 2000). For urban applications, where the EPS is required to support roadways and highways, it is recommended that EPS19, or higher, be used (Bartlett et al. 2000). It is important to select an EPS density with a sufficiently high Young's modulus so as to prevent short-term and creep damage to the EPS from live and dead loads. Figure 3 shows the relation between Young's modulus and EPS density for samples of EPS tested by the University of Utah with specimens larger than 50mm.

Recent field monitoring studies of roadways show that if the compressive (i.e., vertical) stress imposed in the EPS block is restricted to the elastic range, any resulting deformation will mostly take place during construction as the overlying loads are applied and that the post-construction deformation (i.e., creep) will be relatively small and within acceptable limits (Negusse and Studelin 2003; Farnsworth et al. 2008). To limit the creep deformation, it is recommended that the vertical stress level from all dead loads (e.g., trench backfill, roadbase, pavement, etc.) should be limited to 30 percent of the compressive strength of the EPS at 5 percent axial strain. In addition to the dead loads, an additional 10 percent vertical stress is

allowed for live loads (e.g., traffic wheel loading). Such criteria have been used widely before and are believed to result in no more than 2 percent creep strain in the EPS in a 50-year period (Draft European Standard, 1998).

A similar approach used in Japan is to limit the vertical stress level from all loads to a value that corresponds to compressive resistance at 1 percent axial strain for the selected EPS density (Miki, 1996). This is the approach used on the I-15 Reconstruction Project and has produced similar long-term performance as the European Standard requirements (Farnsworth et al. 2008).

In addition, a 4 to 6-inch reinforced concrete slab is often poured atop the EPS for roadway applications where the EPS and overlying pavement section must support heavy truck traffic. Further guidance regarding the design of the EPS in conjunction with pavement systems can be found in NCHRP Web Document 65.

Poisson's Ratio

In the elastic range, Poisson's ratio for EPS is typically relatively low with values of about 0.1 for EPS19 (Negusse, 2006). However, in the plastic range (i.e., the large strain range induced by PGD), Poisson's ratio is slightly negative (it should be noted that Poisson's ratio is an elastic property and is not strictly applicable to the plastic range where the dilation angle can also be negative and produce volumetric contractive behavior). Large strain unconfined axial compression tests of 24-inch (608 mm) block specimens tested at the University of Utah revealed that the sample sides developed a slightly concave rather than a convex (i.e., bulging) shape upon loading. This behavior indicates that the samples had slightly contracted in the lateral direction during axial compression, which implies a slightly negative Poisson's ratio in the plastic range. This slightly inward deformation of the samples results from the collapse of the EPS cellular fabric as the block is loaded to higher stress levels.

Strain Rate Effects

The behavior of EPS geofoam is strain rate dependent, particularly in the plastic range. As the strain rate increases, higher compressive resistance develops (Figure 4) (Duskov, 1997). The compressive resistance at large strain increases by about 15 percent when the strain rate is increased from 1 mm/s to 100 mm/s (Figure 4). This effect should be considered for applications where the EPS is rapidly loaded, such as that resulting from PGD where the loadings are measured in milliseconds.

Strain Hardening

In addition, EPS shows a nonlinear strain hardening behavior with increasing strain (Figure 5). After yielding at about 2 percent strain, there is local collapse of the cellular structure. Continued compression leads to collapse of neighboring EPS cells and the initial failure zone spreads (Duskov, 1997). When most of the air has been removed from the collapsed zone, additional compressive resistance is provided by plastic-to-plastic contact within the EPS,

which produces strong strain hardening behavior. This stiffened behavior starts about 50 percent axial strain and becomes very pronounced at 70 percent axial strain (Figure 5).

The strain field that develops around a pipe pushed into EPS is complex and very non-uniform. The strain gradient is highest near the EPS-pipe contact and decreases at distances away from the pipe (Figure 6). In addition, localized shearing of the EPS block corners occurs adjacent to where the pipe is contacting the EPS at a location where the shear stresses are maximized. However, the compressional zone in the EPS directly above the pipe continues to resist vertical load with increasing displacement (Figure 7). This strain hardening behavior can be deleterious to applications that require a significant amount of compression in the EPS during PGD. Thus, it is recommended that this strain-hardening behavior be avoided when using EPS as a compressible inclusion in the sidewalls or bottom of a trench undergoing large amounts of PGD. Such strain hardening may significantly increase the bending and shear stresses that develop in the pipe system.

Interface Shear Strength

Interface shear strength between geofoam block and between geofoam and bedding sand are shown in Figure 8 (Bartlett et al. 2000). It can be seen that coefficients for both the geofoam-to-geofoam and geofoam-to-sand interfaces decrease with increasing normal stress (Figure 8). These test results are for a range of normal stresses typical for shallowly buried pipe. The somewhat lower coefficients for the sand-to-geofoam interface imply that failure at the interface would be localized and probably occurring within the sand. As the normal stress increases, the failure transitions into the geofoam itself; resulting in the lower frictional interaction coefficient. Also shown is the lower bound envelope for the coefficient of friction for cases where this parameter governs the design.

PIPELINE PROTECTION USING EPS GEOFOAM

Introduction

Because of its light-weight and relatively compressible nature, geofoam can be used as backfill and cover material to protect pipelines from the deleterious effects of permanent ground displacement (PGD). PGD is any vertical and/or horizontal displacement of the soil resulting from seismic events or mass movement processes. Faulting, tectonic deformation, subsidence, liquefaction, land sliding, etc., are examples of processes that produce PGD.

The characteristics of EPS applicable to pipeline protection are its extremely low mass density (12 to 45 kg/m³) and its moderately high compressibility when compared with typical granular backfill materials. When used as a lightweight backfill or in pipeline cover system, geofoam can minimize the vertical and horizontal stresses imposed on the buried pipelines. The lightweight nature of geofoam has been used to reduce soil pressures on buried culverts (Sun et al. 2009) and to decrease static lateral earth pressure against buried walls (Negussey and Sun, 1996). It can also be used to mitigate ground settlement impacts to buried structures due to the

construction of nearby embankments (NRRL, 1992; Sanders, 1994; Duskov, 1997; Bartlett et al., 2000).

When used a compressible inclusion, geofam can reduce the vertical and horizontal earth pressures on pipelines, culverts, retaining and buried walls due to its relatively low stiffness (Horvath, 1991, 1995, 1996b, 1997). The concept of using EPS as a “compressible inclusion” that is placed between a buried structure, such as a pipeline, and the adjacent or overlying soil mass was conceptualized in the 1920s (Horvath, 2008). A compressible inclusion is created when a less stiff material (i.e., inclusion) is placed within the soil or adjacent to the structure or pipeline. As the soil load is applied, the inclusion compresses and produces a significant redistribution of shear and normal stresses in the adjacent soil as the soil’s internal shear strength is mobilized. This concept can be used to reduce horizontal and vertical earth pressures, depending on where the compressible inclusion is placed, its thickness and its stiffness. For example, compressible inclusions have been created in the backfill of retaining and basement walls to reduce horizontal earth pressures (e.g., Reeves and Filz, 2000). Recently, Bathurst and Zarani (2006, 2007) have used shake table tests and finite difference modeling to evaluate EPS’s effectiveness in reducing dynamic lateral earth pressures that develop behind relatively rigid retaining wall systems subjected to strong earthquake shaking.

Several researchers have developed methods for evaluating pipelines subject to horizontal displacement in earthen backfill materials. Horizontal PGD may result from strike-slip faulting, liquefaction-induced lateral spreading and land sliding and other types of mass movement. These mechanisms have been researched by Newmark and Hall (1975), Wang and Yeh (1985), and Kennedy et al. (1979), and solutions have been developed for buried steel pipelines undergoing horizontal and/or longitudinal deformation. In addition, the finite element method (FEM) has been used widely to model horizontal PGD and estimate its effects on steel pipelines (Takada, 2001 and Desmond et.al, 1995). More recently, Karamitros et al. (2007) have used the FEM to develop a strike-slip model for pipelines crossing active faults based on the earlier work of Wang and Yeh (1985) and Kennedy et al. (1979).

Limited research has been done to evaluate buried pipeline systems subject to vertical PGD such as that caused by normal faulting. This topic is important in earthquake prone areas where extensional tectonics can cause predominately vertical displacement on normal fault such as in the U.S. intermountain west. For vertical PGD, ASCE TCLLE (1985), MCEER (2005) and ASCE-ALA (2001-2005) recommend using the Newmark and Hall (1975), or Kennedy et al. (1979) or finite element methods (FEM). However, most researchers agree that such methods are better suited for horizontal movements and for cases where the pipeline is buried sufficiently deep so as not to reach the ground surface during vertical PGD event. Trautmann and O’Rourke (1985) have shown that the horizontal and vertical movements of pipes through soil are essentially the same as that of plates undergoing that same movement. Cheuk et al. (2005) later confirmed these findings and develop soil-pipe interaction (i.e., Winkler) springs for use in FEM modeling. The Cheuk et al. (2005) approach is based on the assumption that the soil and structure interact as a non-damped uncoupled spring (Winkler, 1867). The soil spring constants are generally calculated from the sectional configuration of the system, dimensions of the

underground structure, stiffness of the soil deposit, direction of loading and the boundary conditions.

Evaluation of EPS Cover Systems in Uplift

Very little research has been done to-date on the design of EPS to protect pipelines from the effects of vertical PGD (e.g., normal faulting). The Trautmann and O'Rourke (1985) soil-pipe springs approach has been recommended by ASCE, MCEER and ASCE-ALA. However, all of these groups conclude that pipeline crossings at normal faults require more investigation. The remainder of this section discusses the use of EPS as a lightweight cover system to protect pipeline from the effects of vertical PGD.

Yoshizaki and Sakanoue (2003), Choo et al. (2007) and Lingwall and Bartlett (2007) have evaluated EPS as a lightweight cover/backfill system for buried pipelines. These studies show that EPS significantly reduces the vertical and horizontal soil pressures acting on the soil-pipeline system as the pipeline undergoes PGD. These reductions are a result of geofoam's extremely low mass density. For example, Yoshizaki and Sakanoue (2003) have shown that the horizontal force on a 100-mm steel pipeline undergoing horizontal PGD is significantly reduced when compared to sand backfill. They conducted horizontal pipe displacement tests in a 2 m (wide) by 2 m (high) by 3.1 m (long) trench box using both geofoam cover systems and conventional sand cover. In these tests, no geofoam was placed along the sides of the pipe. Force-displacement measurements were taken as the pipe was displaced a maximum distance of 150 mm. For the geofoam cover systems, the peak horizontal force on the pipe was reduced by 40 to 60 percent compared with a typical sand cover. In addition, Yoshizaki and Sakanoue (2003) found that the resistance of pipeline elbows subjected to PGD could be significantly improved by using EPS backfill placed around the pipe elbow.

More recently, Choo et al. (2007) have shown that when geofoam is placed in the cover and trench sidewalls, it significantly reduces soil-pipeline interaction forces for high-density polyethylene (HDPE) pipe. The conclusions were based on 12 experiments and subsequent analyses from centrifuge tests performed on and various geofoam remediation strategies. The strategies were successful in reducing the peak transverse lateral force at the soil-pipe interface by as much as 80 to 90 percent, depending on the block placement configuration. The reduction in the lateral force led to a 45 to 60 percent reduction in the pipe bending strain when compared with systems without EPS remediation. In addition, the EPS systems reduced the axial strain in the pipe by approximately 15 to 30 percent. (This reduction is a result of the lower frictional force that acts along the pipe due to the low mass density of the EPS when compared with that of soil. The reduced weight of the cover system results in lower normal stresses acting on the pipe's surface at its interface with the soil/geofoam; hence the frictional force will also be reduced as the pipe attempts to move along this interface. The net result is lower axial strain in the pipe because of the pipeline is freer to move longitudinally along this interface.)

Lingwall and Bartlett (2007) have evaluated numerically the benefits of an EPS cover system for protecting a 0.6-m diameter steel pipe that crosses the Salt Lake City, Utah segment of the Wasatch fault (Figure 9). The cover configuration shown in this figure is best for

locations where the pipe is located on the downthrown side of the fault and where the relative vertical displacement will cause the pipe to uplift into the cover system. The numerical evaluations suggested that a lightweight geofoam cover system offers substantial benefit in improving the expected uplift performance of steel pipelines crossing normal faults. The numerical results suggest that when compared with a conventional sand cover, the EPS cover can undergo approximately 4 times greater vertical displacement before pipe yielding was predicted by the model (Lingwall and Bartlett, 2007). The modeling results suggest that some benefit is gained by placing EPS under the pipe on the upthrown side of the fault to provide a cushion in the trench bottom. It was also recommended that for fault systems with both horizontal and vertical components (i.e., oblique slip faults), additional benefit is gained by placing an inverted trapezoid of EPS atop the pipe. The width of the trapezoid should increase upward and reach its maximum width just below the surface or pavement system.

Subsequently, an EPS cover system similar to that of Figure 9 was constructed atop a 0.6-m diameter steel pipeline on the downthrown side of the Salt Lake City segment of the Wasatch fault. Figure 10 shows the placement of the EPS block in the slot trench atop the pipe, and Figure 11 shows the placement of the roadway system atop the slot trench. It is anticipated that during fault offset, the slot configuration will allow the pipe to uplift vertically in the slot created by the EPS block. As the EPS is compressed, the expected failure of the cover system is an interface sliding failure with sliding occurring between the sides of the geofoam block and the adjacent sidewalls of the trench. It is expected that the asphalt pavement will be damaged by this uplift, but this consequence was deemed acceptable by the project team and the Utah Department of Transportation, which owns and maintains the roadway.

Field Uplift Test of EPS Cover System

After the construction of the cover system shown in Figures 10 and 11, full-scale field testing was done on a similar cover system to further evaluate its performance in uplift (Lingwall, 2009). Two full-scale tests were performed: (1) EPS cover system test and (2) native soil backfill test and where the second test served as a baseline for comparison with first test. A profile sketch of the tested EPS cover system is shown in Figure 12. To construct this test, the trench was over-excavated and the 1-foot (0.3-m) diameter steel pipe was placed in bedding sand. The crane rigging was positioned 3.5 feet (1.07 m) from each end of the 15-foot (4.57 m) long strand of pipe and maintained in a vertical orientation throughout backfill placement and compaction. During the construction of this trench, the clayey native soil on the sides of the trench held a vertical cut and geofoam block were placed against the trench sidewalls. However in some places, the trench walls did not fit tightly against the geofoam blocks. In these locations, bedding sand was used to fill the gap the blocks and trench side walls. To complete the EPS cover system, a pre-poured 6-inch (152 mm) reinforced concrete load distribution slab was placed atop the EPS29 and covered by 16 inches (52.5 mm) of granular compacted fill. Figure 13 shows the pipe and EPS block exposed in the ends of the trench prior to starting the uplift test.

Instrumentation for this test consisted of total pressure cells placed atop the EPS and string pod potentiometers attached to rebar tell-tales to measure displacement. The string pods were suspended by 2 by 6-inch (51 mm x 152 mm) lumber frames that were founded outside the zone

of uplift so that absolute uplift measurements could be made. For each uplift test, a 100-ton (996 kN) truck mounted crane was used and the rigging was connected to the inline tension load cell to measure the total uplift force that developed in the cable. All instrumentation from the load and pressure cells and the potentiometers were connected to a datalogger for continuous data acquisition. During the test, the pipe was uplifted as slowly as possible to obtain a reasonable record of the force-displacement history. Uplift continued until the pipe had completely uplifted through the cover system (Figure 14).

A comparison trench-cover system was constructed using compacted native soil in place of the EPS and load distribution slab as a baseline to compare the results of the EPS system. This was also similarly instrumented and brought to failure in uplift. This comparison showed that the EPS cover system was reasonably efficient in reducing the total uplift force (Figure 15). The native soil backfill system reached a peak force of 520 kN at a displacement of 0.06 m. In contrast, the EPS cover system reached a peak force of 136 kN at a displacement of 0.18 m. Thus, the total uplift force had been reduced approximately 73 percent by using the EPS cover system instead of native soil backfill. This reduction of the peak uplift force and its occurrence at larger displacement was suggested by the prior numerical modeling (Lingwall and Bartlett, 2007) and confirmed by this experiment. Additional numerical modeling of these and other tests is ongoing to evaluate further the uplift tests and continue to develop methods for estimating the reduction of bending and longitudinal stresses in buried steel pipelines covered by EPS and subject to vertical PGD (Lingwall, 2009).

Evaluation of EPS Compressible Inclusion in Trench Sidewalls

In addition to the field uplift tests, a series of horizontal pipe displacement tests were conducted in a trench box constructed at the University of Utah. The objective of this program was to evaluate the most efficient compressible inclusion configuration for pipe undergoing horizontal PGD where the relative motion of the pipe causes it to move into the trench sidewalls. The box's overall dimensions are: 17.5 feet (5.34 m) long, 6 feet (1.83 m) wide and 6 feet (1.83 m) high (Figure 16). The box is constructed of ¼-inch (6.35 mm) thick steel plates. The horizontal load capacity of the box is approximately 111 kN. Both ends of the trench box were reinforced and braced with structural steel angle and channel sections to withstand the forces involved in the experiments. The end walls of the trench box were heavily reinforced to minimize the reaction deflections of the ram against the wall. A reinforced door was constructed on one end, which allowed side entry into the backfill compartment. The top of the box remained open; thus allowing for the loading, placement and compaction of sand in the backfill compartment. A steel partition wall separates the interior of the box, the smaller compartment for the load device (actuator) and a larger, backfill compartment for the pipe, geofoam and sand backfill. A 6-foot (1.8 m) long strand of 171.5 mm OD steel pipe can be pushed horizontally via push rods that connect the pipe and the actuator via holes in the partition wall between the compartments (Figure 16).

The trench box testing program consisted of 4 tests that used differing backfill/EPS configurations. The first test was configured with a single 24 x 24 x 72 inch (610 x 610 x 1828 mm) block of EPS15 that was placed parallel to and immediately adjacent to the pipe. This block

was positioned so that the center elevation of the pipe was at the center elevation of EPS block and the remaining compartmental space was filled in with compacted sand backfill. The pipe was subsequently pushed horizontally into the EPS block and force, displacement and pressure measurements were obtained (Lingwall, 2009). The second test was a baseline test using sand only and was used for comparison purposes. The third test used two 24 x 24 x72 inch (610 x 610 x 1828 mm) EPS15 blocks placed parallel to the pipe at the center elevation of the pipe and the pipe was pushed into an inclusion that consisted of two block. (The rationale for this configuration was to see if the thickness of the compressible inclusion had a significant influence on the load-displacement behavior. It was believed that a thicker compressible inclusion would allow for a softer initial loading and delay the strain hardening behavior that occurs in the EPS at larger strain.) The fourth test did not use a compressible inclusion; but instead made use of a light-weight cover and a pipe that was buried with minimal sand cover (Figure 17). This test sought to reduce the resistance to horizontal displacement by minimizing the weight of the overlying cover. Because lower vertical stress is present in this configuration, the horizontal resistance of sand placed adjacent to the pipe would be reduced significantly, allowing the pipe to displace easily through the adjacent sand and reduce the total force imposed on the pipe.

As expected, test II (sand backfill only) had the stiffest initial response to pipe movement, due to its relatively high stiffness when compared with EPS15. However, test II also had a lower peak force when compared with tests I and III that included the EPS compressible inclusions. The peak displacement from tests I and III had peak loads that occurred at displacements that were approximately 2 to 3 times greater than the sand backfill case (test II). For application purposes, this means that these systems mobilize more force, albeit at larger displacement, than the sand backfill case, which is not a favorable result for pipes that undergo large horizontal displacement into the sidewalls of the trench (e.g., strike-slip displacement). However, there is still application for cases where the expected displacements are small.

Fortunately, the force-displacement behavior measured for test IV is much more favorable from an application standpoint. This test shows an initially stiff behavior followed a relatively flat force-displacement response. The light-weight cover of this system produces the lowest peak force of all tests and maintains a relatively low resistance for considerable displacement. Thus, it was concluded that the lightweight cover concept offers the best alternative, rather than the compressible inclusion concept, for protecting pipe for large PGD resulting from strike slip faults.

CONCLUSIONS

A light-weight cover system of EPS geofoam offers significant benefits to protecting pipe from the effects of vertical PGD such as normal faulting. Because of its extremely low mass density, a geofoam cover system significantly reduces the vertical and/or uplift forces on a pipe system undergoing vertical PGD. Full-scale testing and numerical modeling have demonstrated that the total force on the pipe is reduced by a factor of about 3 to 4 when compared with a trench backfilled with soil.

In addition, it was found that EPS geofoam behavior in compressive loading against a trench sidewall is highly non-linear and that the EPS experiences significant strain hardening at higher compressive strains. The localized strain field that develops around a pipe as it is pushed into EPS is complex and the strain gradient is highest near the pipe and diminishes away from the pipe. In addition, localized shearing of the EPS block occurs near the corners of the block where shear stresses are maximized. Although the EPS is successful in providing some benefit when used in the sidewalls of the trench, it has limited value because relatively high forces are realized at larger displacement. Based on this, it was concluded that EPS used as a compressible inclusion in the sidewalls or bottom of a trench has limited value in reducing the forces that develop on the pipe for systems undergoing a significant amount of PGD. As the pipe is pushed into the EPS, a localized strain hardening zone develops within the EPS near the contact zone and such behavior can significantly reduce the effectiveness of the compressible inclusion. Therefore, it is recommended that significant strain-hardening behavior be avoided when using EPS as a compressible inclusion in the sidewalls or bottom of a trench.

However, an EPS cover system constructed atop a pipe that undergoes horizontal PGD is beneficial, even for strike-slip faulting. Tests performed by several authors suggest that the total force on the pipe can be reduced by a factor of about two, even if the pipe is pushed horizontally into a sand backfill. (This latter benefit occurs because the EPS light-weight cover system significantly reduces the vertical stresses on the pipe and sand, which in turn reduce soil's resistance to horizontal pipe displacement. Thus, it appears that the application of light-weight cover systems, such as EPS, have benefit for pipes undergoing primarily horizontal PGD.

REFERENCES

- Aaboe, R. (2000). "Evidence of EPS long-term performance and durability as a light weigh fill," Transportation Research Board 79th Annual Meeting, January 9-13, 2000, Washington, D.C.
- American Lifeline Alliance – ASCE, (2005), Guidelines for the Design of Buried Steel Pipelines, July 2001 (with addenda through February 2005), ASCE.
- American Society of Civil Engineers (ASCE), (1984), Guidelines for the Seismic Design of Oil and Gas Pipeline Systems, Technical Council on Lifeline Engineering, Committee on Gas and Liquid Fuel Lifelines, ASCE.
- Bartlett, S. F., Negussey, D., Kimball, M. (2000), "Design and Use of Geofoam on the I-15 Reconstruction Project," Transportation Research Board, January 9th to 13th, 2000, Washington, D.C., 20 p.
- Cheuk, C.Y. White, D.J. and Bolton, M.D. (2005). "Deformation mechanisms during uplift of buried pipes in sand". 1st International Conference on Soil Mechanics and Geotechnical Engineering, September. (2) 2005, Osaka, Japan, 1685-1688.

Choo, Y. W., Abdoun, T. H., O'Rourke, M. J. and Da, H. (2007). "Remediation for buried pipeline systems under permanent ground deformation," *Soil Dynamics and Earthquake Engineering* 27 (2007) 1043-1055.

Desmod TP, Power MS, Taylor CL, Lau RW. "Behavior of large-diameter pipeline at fault crossings." *ASCE,TCLEE* 1995; (6):296 –303.

Draft European Standard, (1998). European Committee for Standardization, Brussels.

Duskov, M. (1997). " EPS as a light-weight sub-base material in pavement structures," Ph.D. Thesis, Delft University of Technology, The Netherlands.

Elragi, A.F. (2000). " Selected Engineering Properties and Applications of EPS Geofoam, Ph.D. Dissertation, State University of New York College of Environmental Science and Forestry, Syracuse, NY.

Elragi, A. F., Negusse, D., Kyanka, G., (2000). "Sample Size Effects on the Behavior of EPS Geofoam," *Soft Ground Technology Conference, Noordwijkwehout, The Netherlands.*

Farnsworth C. F., Bartlett S. F., Negusse, D. and Stuedlein A. (2008). "Construction and Post-Construction Settlement Performance of Innovative Embankment Systems, I-15 Reconstruction Project, Salt Lake City, Utah," *Journal of Geotechnical and Geoenvironmental Engineering, ASCE* (Vol. 134 pp. 289-301).

Frydenlund, T. E. and Aaboe, R. (1996). "Expanded Polystyrene -The Light Solution," *Proceedings of the International Symposium on EPS Construction Method, Tokyo.*

Horvath, J. S. (1991). "Using geosynthetics to reduce surcharge-induced stresses on rigid earth retaining structures", *Transportation Research Record No. 1330*, Transportation Research Board, Washington, D.C., U.S.A., pp. 47-53.

Horvath, J. S. (1995). Geofoam Geosynthetic, Horvath Engineering PC, Scarsdale, New York, 217 p.

Horvath, J. S. (1996a). "Geofoam Geosynthetic: Past, Present, and Future," *Electronic Journal of Geotechnical Engineering.*

Horvath, J. S. (1996b). "The compressible inclusion function of EPS geofoam: an overview." *Proc. Intl. Sym. on EPS Construction Method (EPS Tokyo '96)*, Tokyo, Japan: 71-81.

Horvath, J. S. (1997). "The compressible inclusion function of EPS geofoam," *Geotextiles and Geomembranes*, 15 (1-3): 77-120.

Horvath, J. S. (2008). "Extended Veletsos-Younan Model for Geofoam Compressible Inclusions Behind Rigid, Non-Yielding Earth-Retaining Structures," *Geotechnical Earthquake Engineering and Soil Dynamics IV, American Society of Civil Engineers Geo-Institute, Sacramento, California, May 18 to 22, 2008.*

Karamitros, D.K., Bouckovalas, G.D., and Kouretzis, G.P. (2007). "Stress Analysis of Buried Steel Pipelines at Strike-slip Fault Crossings". *Soil Dynamics and Earthquake Engineering*, (27), 200-211.

Kennedy, R.P., Darrow, A.C., Short SA. (1979). "Seismic design of oil pipe systems." *Journal of Technical Councils of ASCE*; 105(TCI):119–134.

Kennedy, R.P., Kincaid, R.H. "Fault crossing design for buried gas oil pipelines." *ASME, PVP* 1983; 77:1–9.

Lingwall, B. (2009). "Protection of Buried Pipelines from Permanent Ground Displacement Using EPS Geofoam," Dissertation, Department of Civil and Environmental Engineering, University of Utah.

Lingwall, B. and Bartlett, S. F. (2007). "Conceptual Design and Modeling: EPS Geofoam Cover System for Buried Pipelines," prepared for Questar Gas Corporation, Salt Lake City, Utah, Aug. 2007, 22 p.

NCHRP Web Document 65 (2004). "Geofoam Applications in the Design and Construction of Highway Embankments," Transportation Research Board Project 24-11, July 2004, 792 p.

Newmark, NM, Hall, W.J. (1975). "Pipeline design to resist large fault displacement." *Proceedings of U.S. National Conference on Earthquake Engineering*; 416–425.

Negussey, D. (2006). "Design parameters for EPS Geofoam." *Soils and Foundations*. Syracuse University, August 2006, Syracuse New York.

Negussey, D. and Sun, M.C. (1996). "Reducing Lateral Pressure by Geofoam (EPS) Substitution". *Proceedings of the 2nd International Conference on EPS*, Tokyo, 1996.

Negussey, D., and Studlein, A. (2003). "Geofoam fill performance monitoring." *Utah Dept. of Transportation Research Div. Rep. No. UT-03.17*, Research Division, Utah Department of Transportation, Salt Lake City, Utah.

Negussey, D., Stuedlin, A. W., Bartlett, S. F., and Farnsworth, C. (2001). "Performance of geofoam embankment at 100 South, I-15 reconstruction project, Salt Lake City, Utah." *Proc., EPS Geofoam, 3rd Int. Conf.*, Salt Lake City, Utah, 22.

Newman, M. P., Bartlett S. F., and Lawton E. C. (2010). "Numerical Modeling of Geofoam Embankments," *ASCE Journal of Geotechnical and Geoenvironmental Engineering*, February, 2010, pp. 290 – 298.

Multidisciplinary Council on Earthquake Engineering Research (MCEER), (1999), Response of Buried Pipelines Subject to Earthquake Effects, MCEER Monograph No. 3.

Miki, G. (1996). EPS Construction Method in Japan. Proceedings of the International Symposium on EPS Construction Method, Tokyo.

Norwegian Road Research Laboratory (1992). "Expanded polystyrene used in road embankments: Design, Construction and Quality Assurance," Form 482E. Oslo.

Reeves, J. N. and Filz, G. M. (2000). "Earth Force Reduction by a Synthetic Compressible Inclusion," Research Report Sponsored by GeoTech Systems Corporation and Virginia's Center for Innovative Technology, Virginia Tech.

Sanders, R. L. and Seedhouse, R. L. (1994). "The use of polystyrene for embankment constructions," Contract Report 356. Transportation Research Laboratory, Crowthorne, UK.

Sun L., Hopkins, T. C., and Beckham, T. L. (2009). "Reduction of Stresses on Buried Rigid Highway Structures Using the Imperfect Ditch Method and Expanded Polystyrene (Geofoam)," Research Report KTC-07-14/SPR-228-01-1F, Kentucky Transportation Center, University of Kentucky, Lexington Kentucky, 49 p.

Takada, S., Hassani, N., and Fukuda, K. (2001). "A new proposal for simplified design of buried steel pipes crossing active faults". Earthquake Engng Struct. Dyn. 2001; (30), 1243–1257.

Trautmann and O'Rourke (1984). "Uplift of buried pipes." Journal of Geotechnical Engineering;

Trautmann and O'Rourke (1984). "Lateral Force-Displacement Response of Buried Pipes." Journal of Geotechnical Engineering.

Wang L.L.R., and Yeh, Y.H. (1985). "Refined Seismic Analysis and Design of Buried Pipeline for Fault Movement." Earthquake Engineering and Structural Dynamics, 13(1), 75-96.

Wang, L.L.R., Wang L.J., "Parametric study of buried pipelines due to large fault movement." ASCE, TCLEE 1995; (6):152–159.

Winkler, E. (1867). Die lehre von elastizität und festigkeit, H. Dominicus, Prague, 182.

Yoshizaki K. and Sakanoue, T. (2003). "Experimental Study on Soil-Pipeline Interaction Using EPS Backfill," Proceedings of the Pipelines 2003 International Conference on Pipeline Engineering and Construction, Baltimore, MD, July 13-16, 2003, pp. 1126-1134.



Figure 1. Placement of expanded polystyrene (EPS) geofoam block around a steel culvert on the I-15 Reconstruction Project, Salt Lake City, Utah.

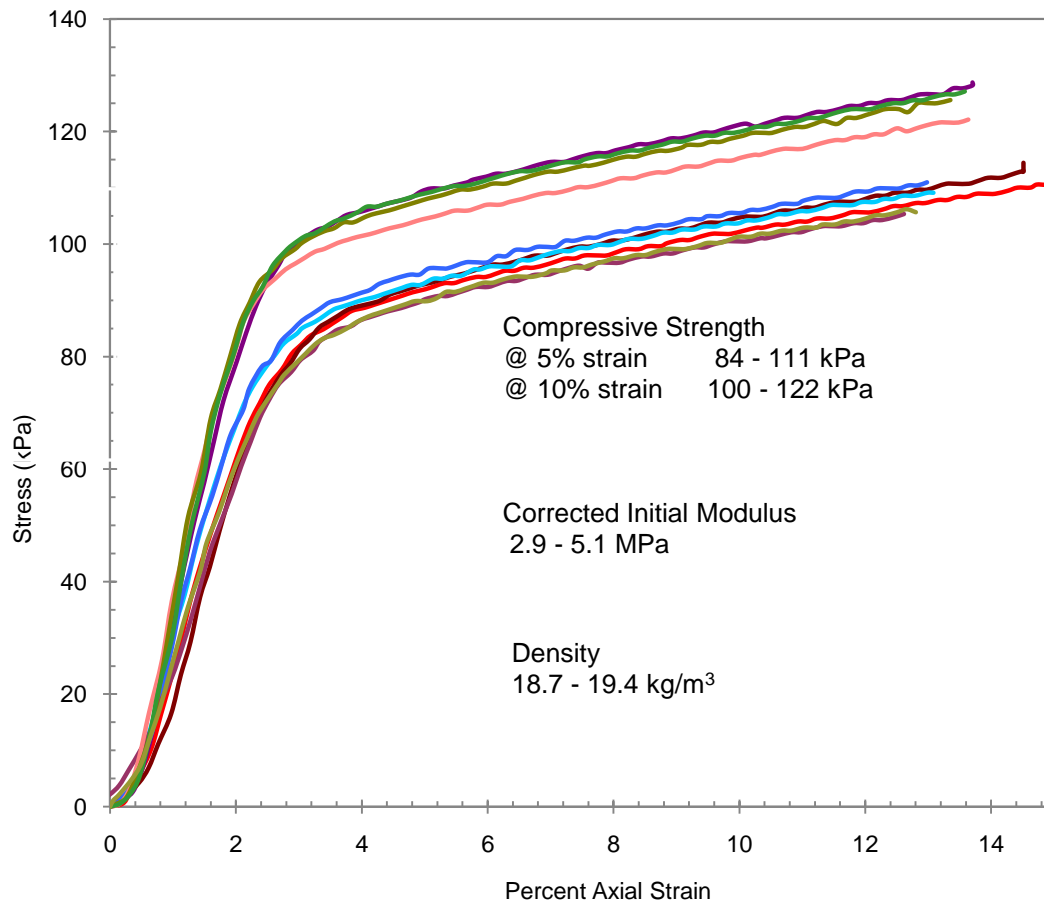


Figure 2. Stress-strain curve for EPS19 50-mm cube samples at 10 percent strain per minute strain rate (Bartlett et al. 2000).

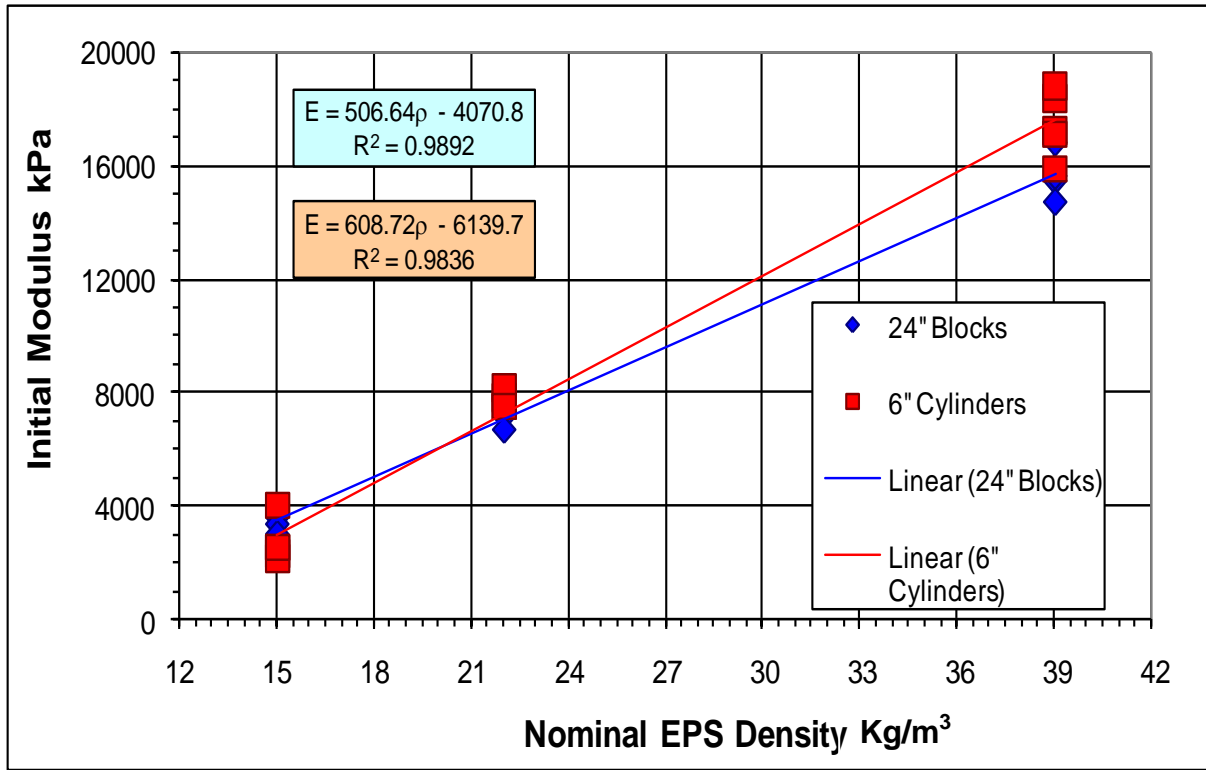


Figure 3. Comparison of initial Young's Modulus for various EPS densities and for 24-inch block and 6-inch cylindrical samples.

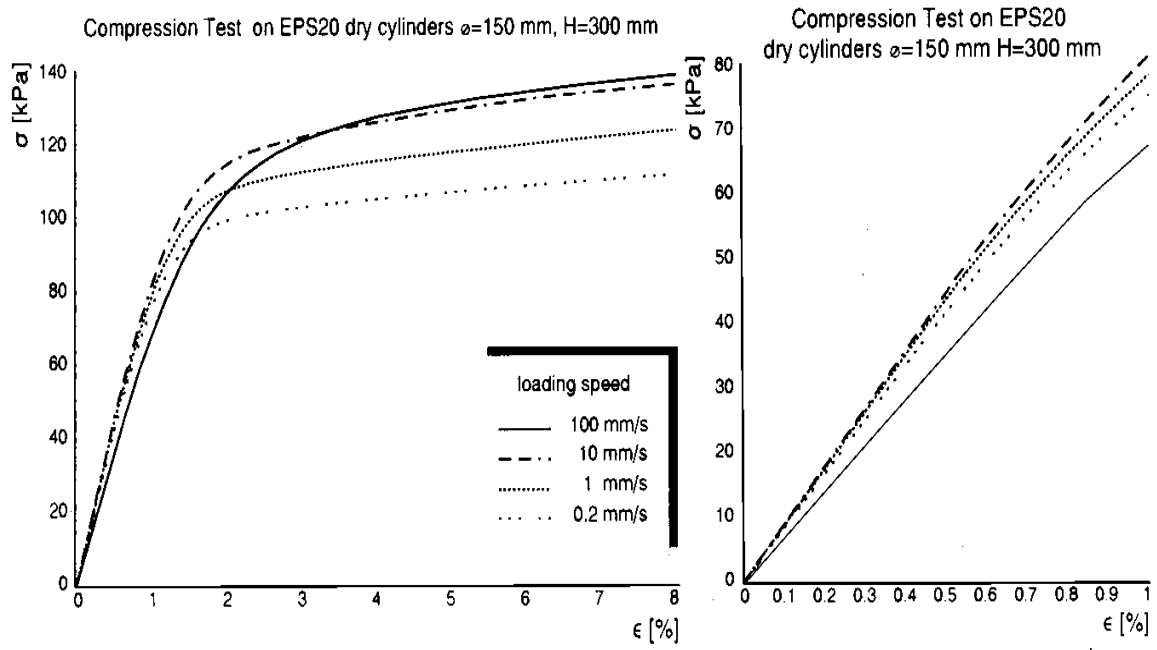


Figure 4. Axial compression strain rate effects for EPS20 (after Duskov, 1997).

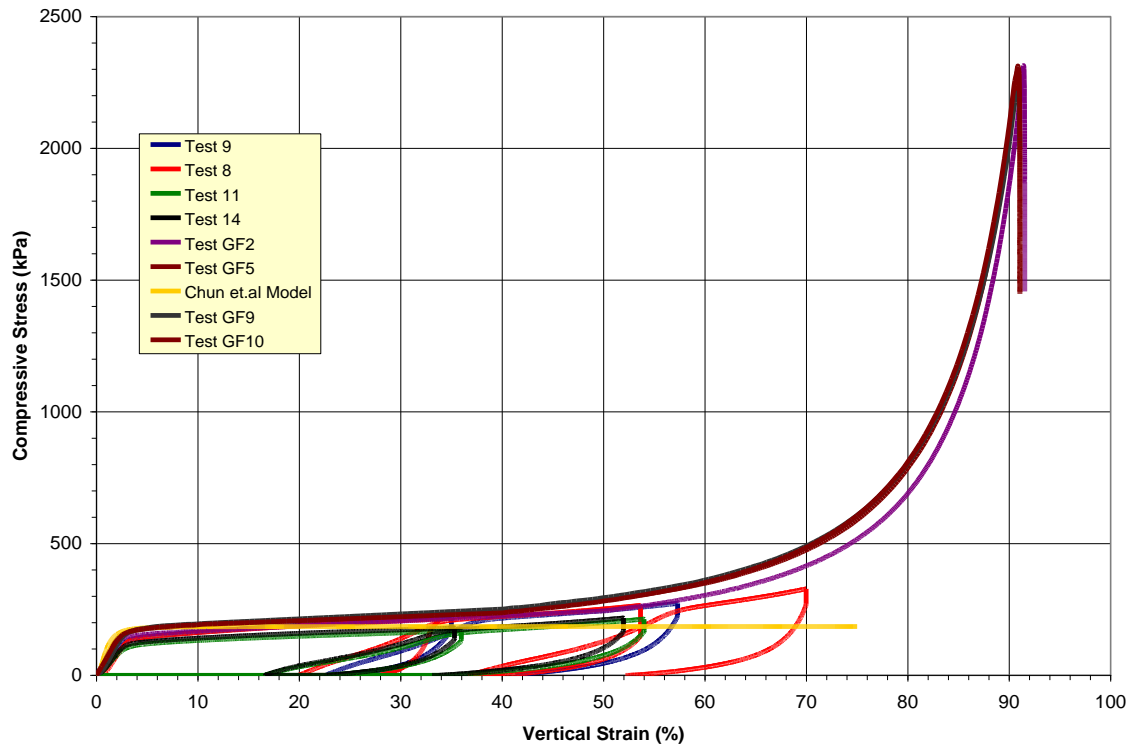


Figure 5. Axial compression stress-strain behavior of EPS22 with strain hardening at high plastic strain.

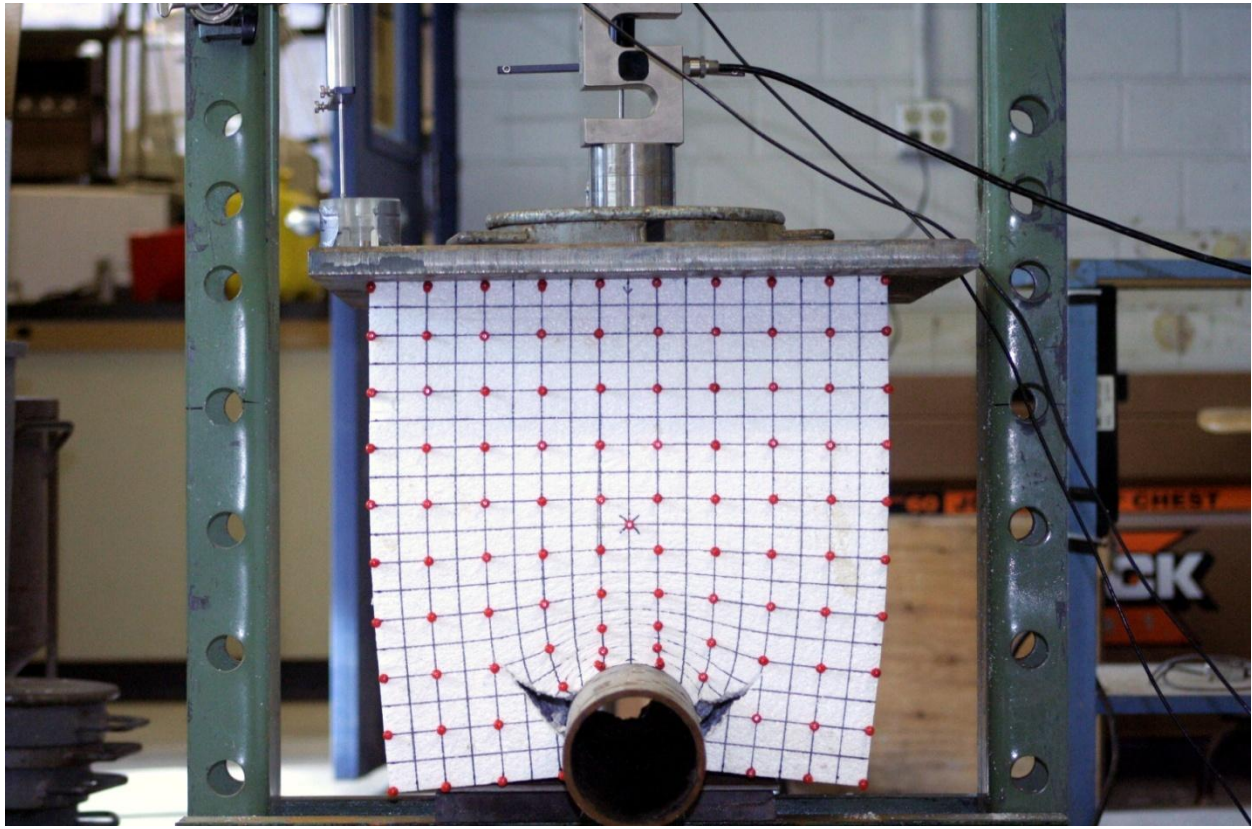


Figure 6. Localized non-uniform strain field and shearing that develops around a 100-mm pipe during compression of EPS15 block after about 90 mm of axial displacement. Original EPS block is a 460 mm cube with an original grid spacing of 25 mm. Dots on the block were originally spaced at 50 mm.

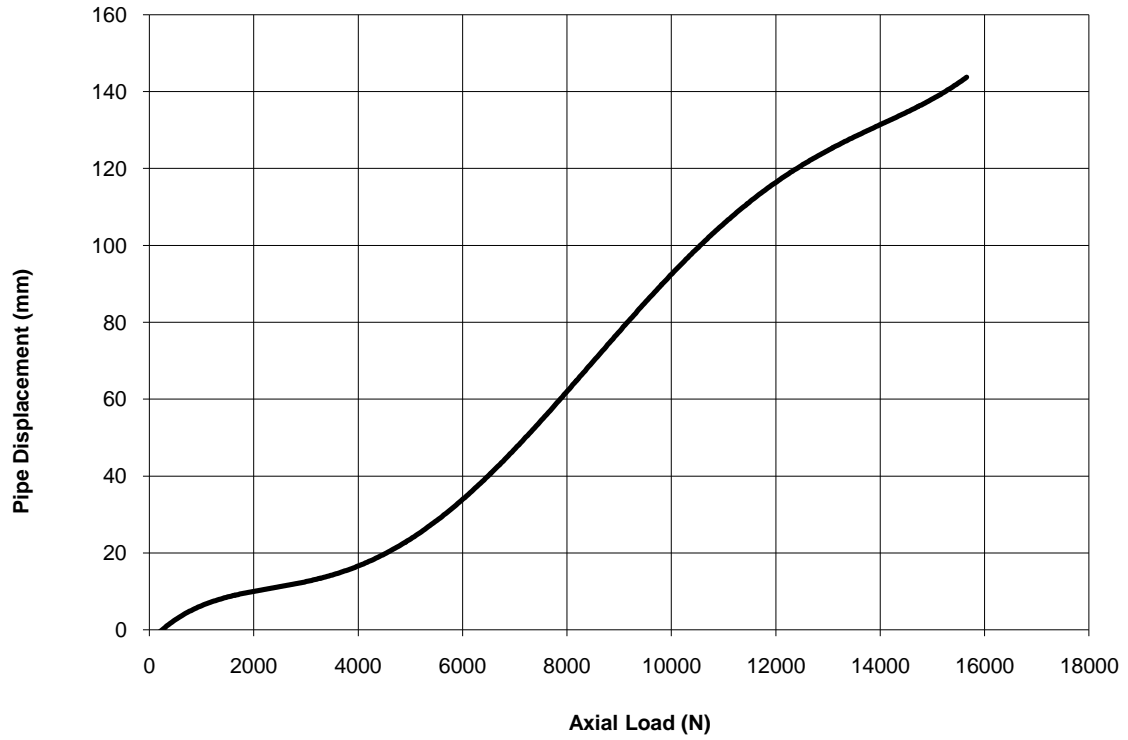


Figure 7. Displacement versus load relation for E1315 block-pipe interaction test shown in Figure 6.

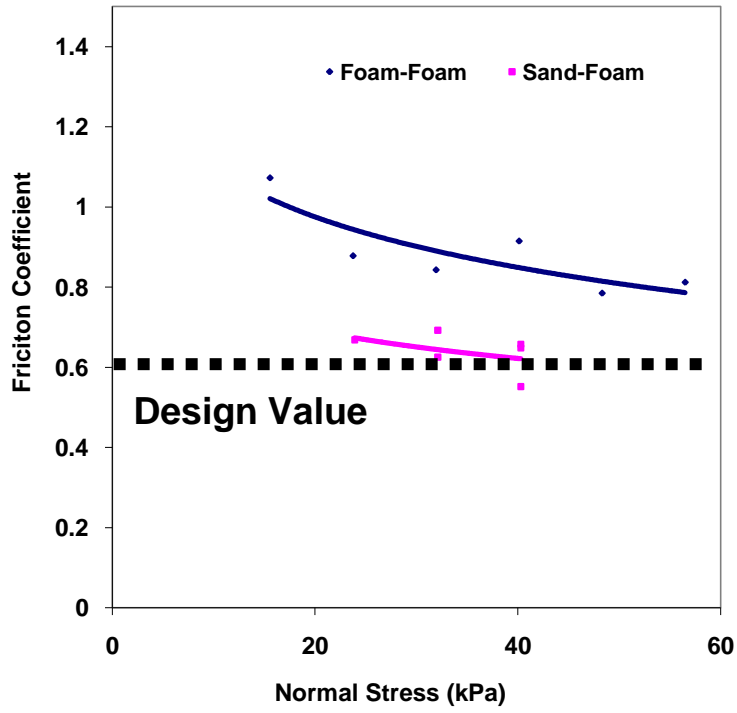


Figure 8. Coefficient of friction for EPS19 and sand and EPS19 to EPS19 surfaces (Bartlett et al. 2000).

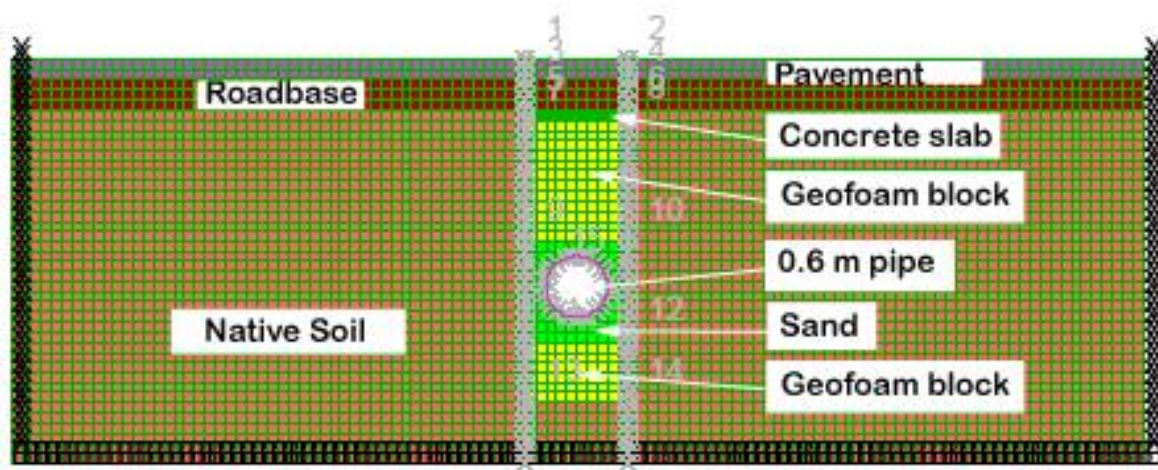


Figure 9. Conceptual EPS cover system for steel pipe undergoing vertical uplift (after Lingwall and Bartlett, 2007).



Figure 10. Placement of geofoam block as a lightweight cover atop a 0.6-m diameter steel pipeline crossing the Wasatch fault zone in Salt Lake City, Utah.



Figure 11. Placement of sand, concrete, roadbase and asphalt atop EPS cover system, Salt Lake City, Utah.

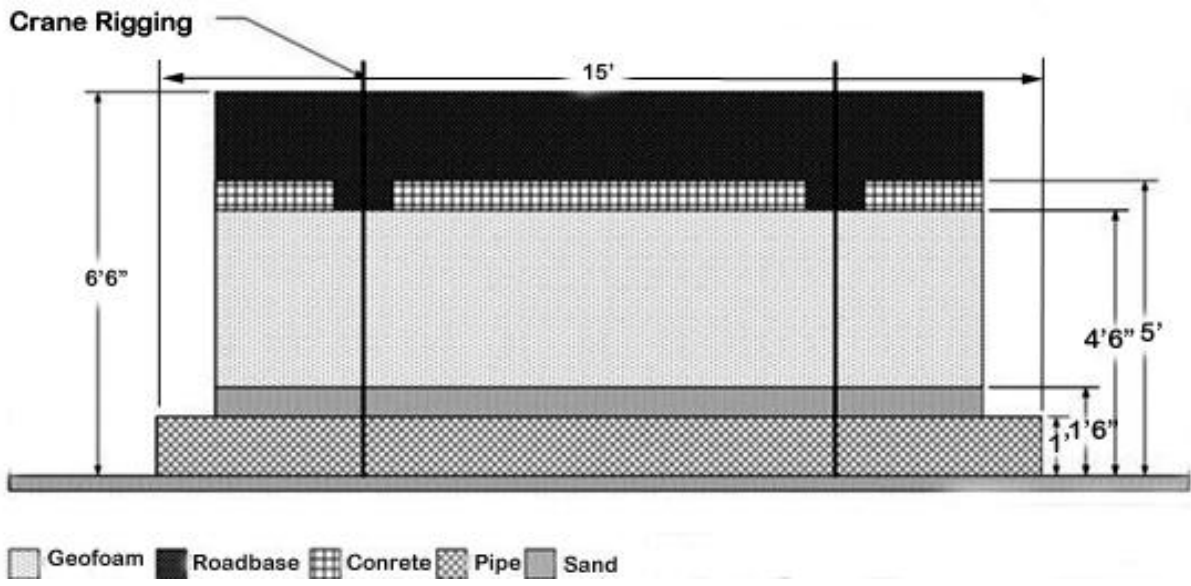


Figure 12. Profile view of EPS cover system field test.



Figure 13. Photograph of the end of trench, pipe, EPS block prior to uplift test.



Figure 14. Photograph of the end of the trench, pipe, EPS block after uplift test.

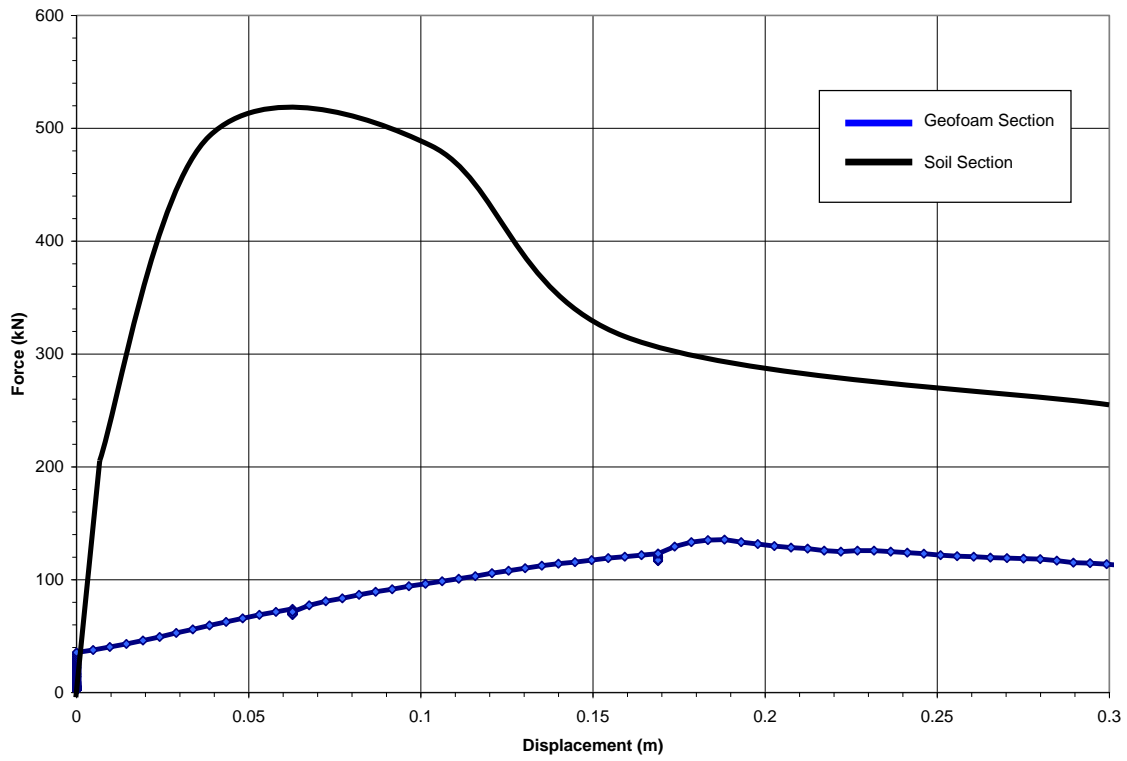


Figure 15. Force-displacement plots for pipe uplift test.

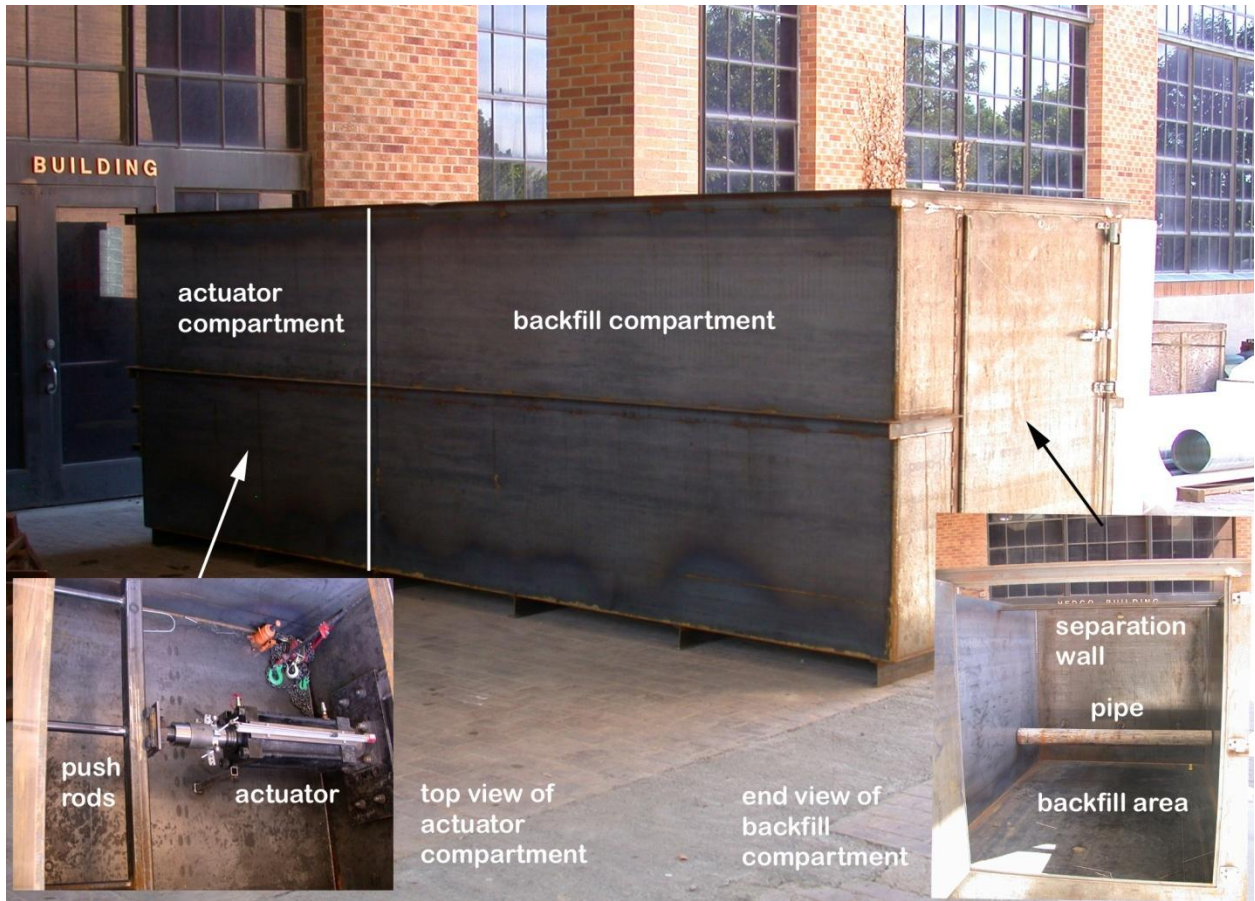


Figure 16. Trench box constructed for horizontal pipe displacement tests.

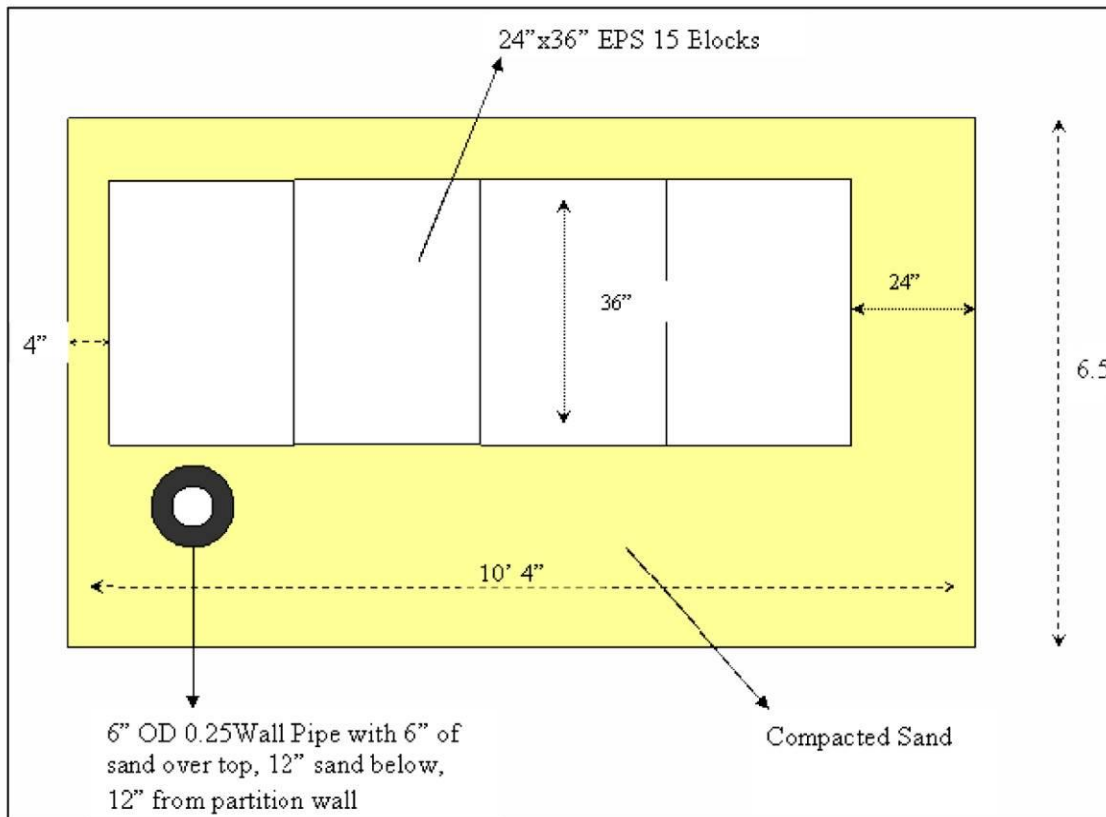


Figure 17. Side view of backfill compartment with EPS cover system used for trench box test IV.

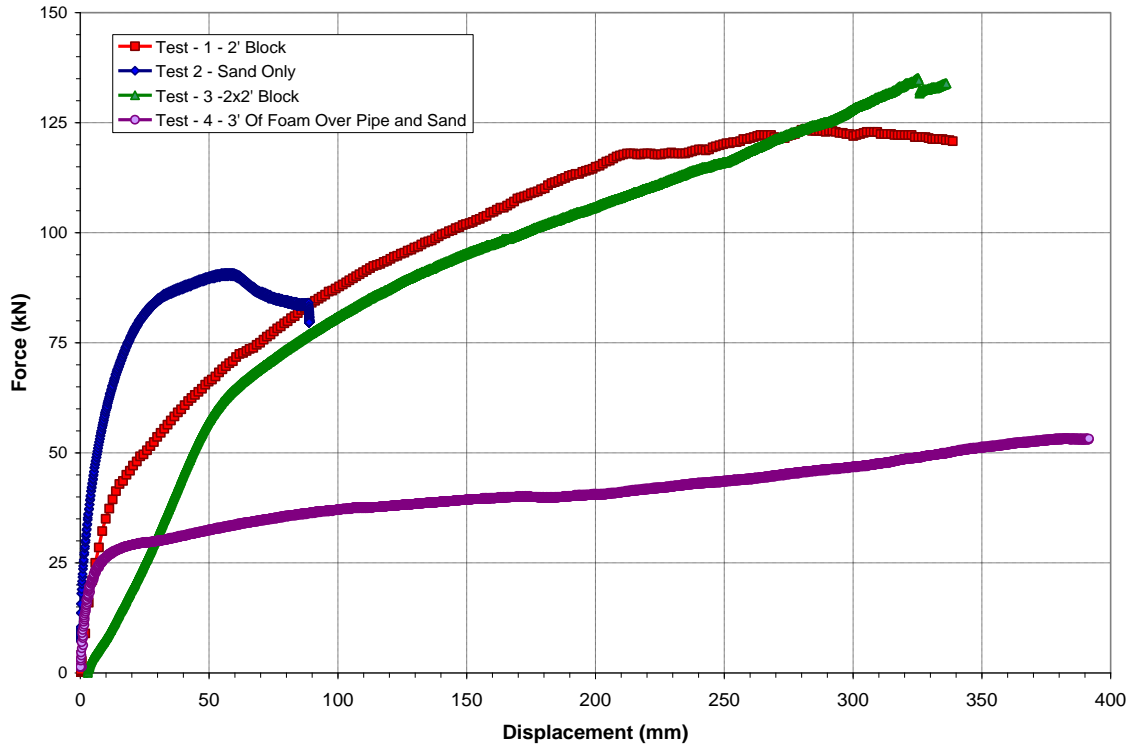


Figure 18. Comparison of force-displacement plots for trench box tests.

